

Chapter 3

Empirical research into improved linear simulation

PART I: Empirical research into improved linear simulation

Due to the relatively short development span of time domain simulation techniques, in particular the Q-ETM software suite, a large amount of empirical research has been done to overcome the resultant lack of application expertise and simulation experience. This lack of application experience is presently a handicap, considering that frequency domain simulation techniques can boast with decades of experience and applications at major testing installations worldwide. The work presented in this Section attempts to clarify some of the uncertainties surrounding time domain simulation, more specifically it addresses input parameters to, and general simulation techniques for, improved time domain response reconstruction. Section 3.1 introduces a procedure to quantify a test rig's input - output repeatability. To the author's knowledge, these repeatability functions are novel. Split-spectra modelling and simulation techniques are introduced in Section 3.2. These functions were developed over a time span of years at LCH Structural Mechanics and Dynamics, by amongst others, the author. Optimal excitation characteristics are briefly discussed in Section 3.3. The procedures developed by the author are based on principles introduced by Barnard [2]. Some of the effects of filter frequencies and bandwidth selections on simulation and modelling results are discussed in Section 3.4. Part I is concluded in Section 3.5 with recommendations for future research.

Chapter 3

Empirical research into improved linear simulation

The most fundamental assumption made prior to modelling and simulating field responses on a test rig is dynamic input-output repeatability. The linear

Due to the relatively short development span of time domain simulation techniques, in particular the QanTiM software suite, a large research effort was engaged to alleviate the resultant lack of application expertise and simulation experience. This lack of application experience is presently a handicap, considering that frequency domain simulation techniques can boast with decades of experience and applications at major testing installations worldwide. The work presented in this Section attempts to clarify some of the uncertainties surrounding time domain simulation, more specifically it addresses input parameters to, and general simulation techniques for, improved time domain response reconstruction. Section 3.1 introduces a procedure to quantify a test rig's input – output repeatability. To the author's knowledge, these repeatability functions are novel. Split-spectra modelling and simulation techniques are introduced in Section 3.2. These functions were developed over a time span of years at LGI Structural Mechanics and Dynamics, by amongst others, the author. Optimal excitation characteristics are briefly discussed in Section 3.3. The procedures developed by the author are based on principles introduced by Barnard [2]. Some of the effects of filter frequencies and bandwidth selections on simulation and modelling results are discussed in Section 3.4. Part I is concluded in Section 3.5 with recommendations for future research.

The performance of the proposed repeatability functions is demonstrated at the hand of four application examples, namely:

- Electro-dynamic linear actuator with an accelerometer mounted directly on the output shaft.
- Vehicle driver unit in a servo hydraulic test rig
- Motorcycle rear wheel road simulator
- Radiator vibration test rig

3.1. Rig repeatability

The most fundamental assumption made prior to modelling and simulating field responses on a test rig, is dynamic input-output repeatability. The linear system identification techniques used within QanTiM are not capable of modelling chaotic or stochastic rig behaviour. It is thus important for the simulation engineer to evaluate rig repeatability prior to modelling and simulation. Two methods are proposed, the first deals with repeatability as a function of excitation frequency, the second attempts to calculate a general repeatability number (scalar).

The test, described in Figure 3.1 makes use of random drive signals created with a prescribed PSD function. The rig is driven five times with the same drive signal while subsequent responses are recorded. A mean response is then calculated from the five response signals. The frequency related repeatability number R_f is defined so that perfect repeatability is achieved at $R_f = 100$. The repeatability vs. frequency plot is useful to identify frequencies that should be avoided while modelling. The repeatability number should provide the engineer with a quick indication of the system's repeatability, and subsequently modelability.

The performance of the proposed repeatability functions is demonstrated at the hand of four application examples, namely:

- Electro-dynamic linear actuator with an accelerometer mounted directly on the output shaft.
- Vehicle damper unit in a servo hydraulic test rig
- Motorcycle rear wheel road simulator
- Radiator vibration test rig

3.1.1. Repeatability function application II Electro-dynamic shaker

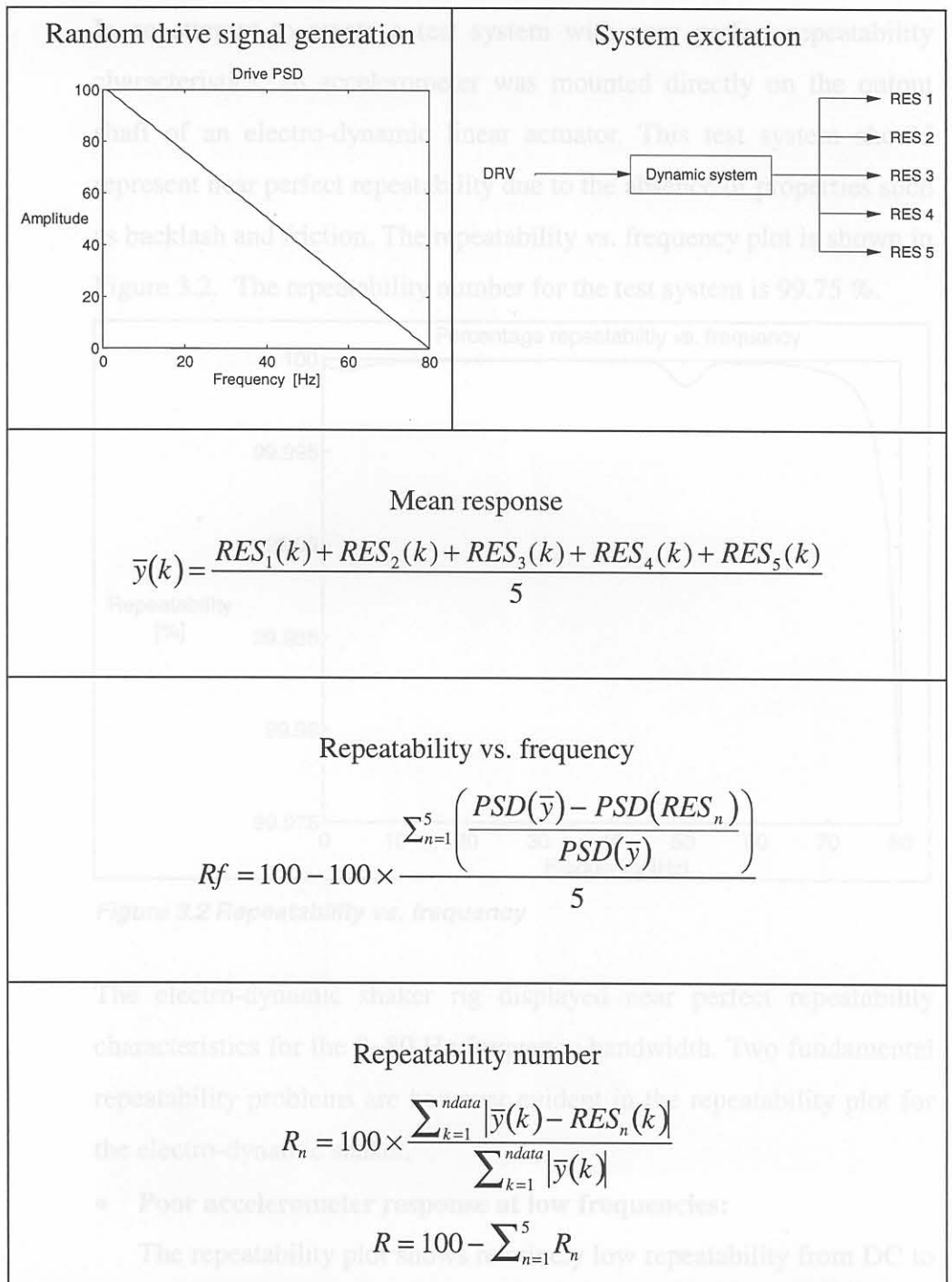


Figure 3.1: Repeatability test procedure

3.1.1. Repeatability function application 1: Electro-dynamic shaker

In an attempt to create a test system with near perfect repeatability characteristics, an accelerometer was mounted directly on the output shaft of an electro-dynamic linear actuator. This test system should represent near perfect repeatability due to the absence of properties such as backlash and friction. The repeatability vs. frequency plot is shown in Figure 3.2. The repeatability number for the test system is 99.75 %.

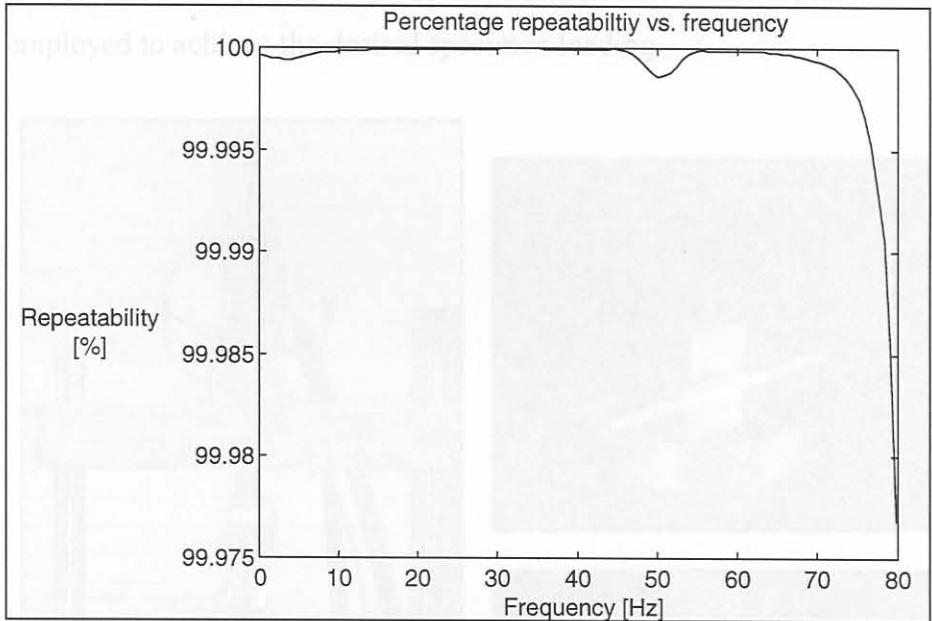


Figure 3.2 Repeatability vs. frequency

The electro-dynamic shaker rig displayed near perfect repeatability characteristics for the 0~80 Hz frequency bandwidth. Two fundamental repeatability problems are however evident in the repeatability plot for the electro-dynamic shaker.

- **Poor accelerometer response at low frequencies:**

The repeatability plot shows relatively low repeatability from DC to 10 Hz. This can be attributed to transducer insensitivity at low frequencies.

- **Power line noise:**

The repeatability plot further shows a decline in the region of 50 Hz. This can be attributed the 50 Hz alternating current power supply.

3.1.2. Repeatability function application 2: Vehicle damper test rig

A single axis servo-hydraulic test rig was set up for qualification testing of heavy vehicle damper units (shock absorbers). The test system is shown in Figure 3.3. The qualification tests required accurate control of specimen loading, which could not be achieved by the analogue servo control system. Response reconstruction techniques were employed to achieve the desired specimen loading.

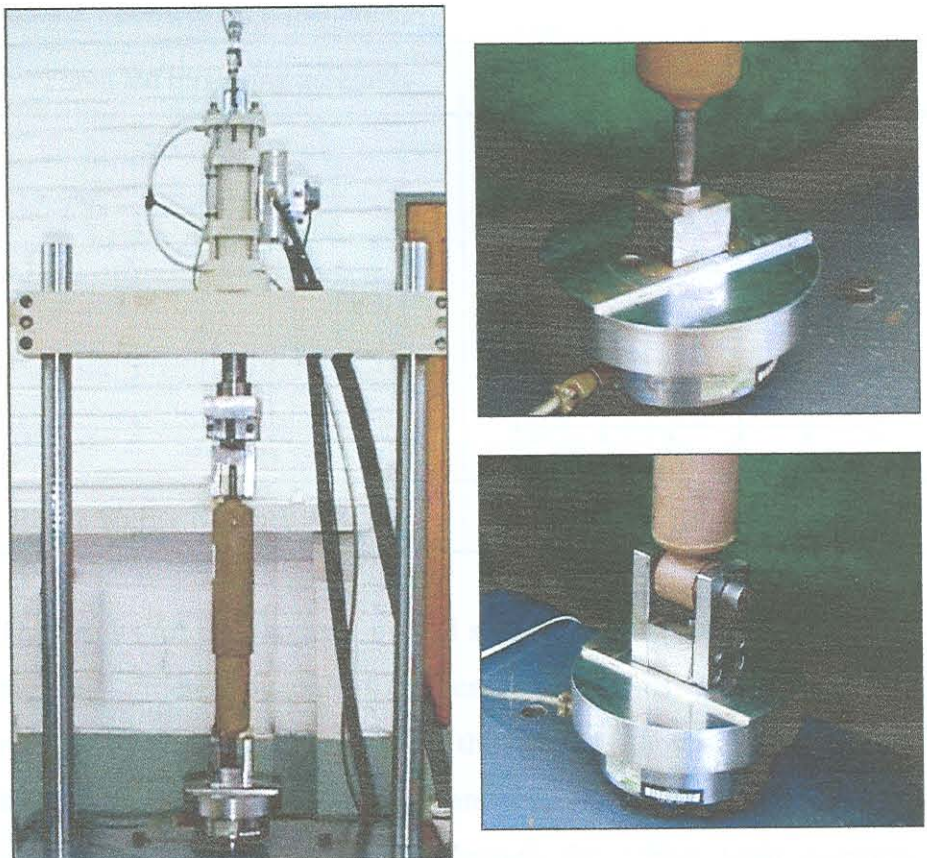
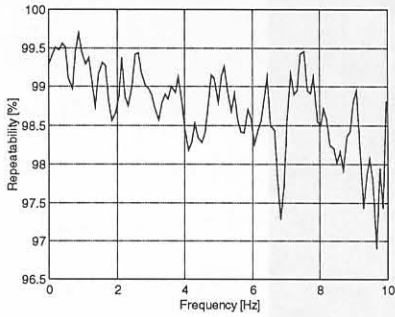
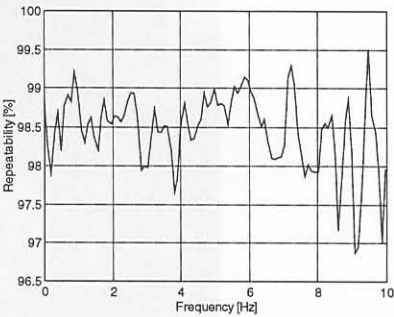


Figure 3.3 Damper test rig

Two damper attachment systems were used (Figure 3.3). The first made use of a threaded connector that rigidly locked the damper to the actuator shaft and the load cell. The second method attached the damper via two rubber bushes. This rubber bush mounting assembly resulted in mechanical play and backlash in the load path.

proposed that the backlash associated with the rubber mounting bushes might be the cause of the unsatisfactory simulation results. The repeatability for each of the two damper mounting methods was assessed with the defined repeatability functions. The damper qualification test prescribed a simulation bandwidth between 0 Hz and 10 Hz. Subsequently the repeatability drive file was randomly generated from 0 to 10 Hz, with a triangular PSD. The repeatability results are presented in Table 3.1 below.

Table 3.1 Damper rig repeatability

Threaded mounting assembly	Rubber bush mounting assembly
	
Repeatability Number = 98.49 %	Repeatability Number = 98.45%

The results for the two tests proved similar, the calculated repeatability numbers differed by only 0.04 percentage points. Furthermore, the repeatability vs. frequency plots for the two tests show similar trends for the 0Hz to 10 Hz simulation bandwidth. The repeatability results indicate that the load response through the rubber bush assembly, including the backlash behaviour, is indeed repeatable. These responses may however be non-linear. Non-linear modelling of the damper unit is presented in Part II of this thesis.

3.1.3. Repeatability function application 3: Motorcycle road simulator

A single axis test rig was set up to simulate road inputs to the rear suspension of a motorcycle. The test rig is shown in Figure 3.4. Input to the system was the actuator displacement drive signals, system responses were recorded from an accelerometer on the wheel spindle, and strain gauges applied to the coil spring.

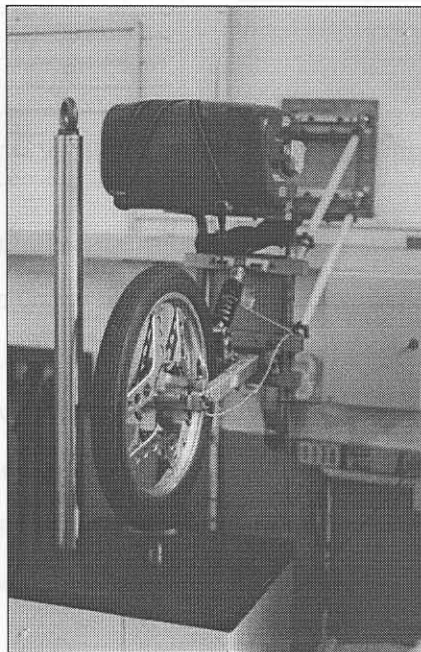


Figure 3.4 Motorcycle rear wheel road simulator

The repeatability drive file was created under a triangular PSD with a bandwidth of 0 Hz to 30 Hz. The repeatability results for the acceleration and strain responses are compared in Table 3.2.

The mounts were fitted to the rigid mounting frame. Play between the mounting pins and the rubber mounts allowed some free movement of the radiator, both vertically and horizontally.

Acceleration responses were recorded on the base of the mounting frame, and on the top tank of the radiator. The repeatability of the base and top tank accelerations are compared in Table 3.3 for a simulation bandwidth of 0 Hz to 25 Hz.

Table 3.2 Radiator test rig repeatability results

Table 3.2 Motorcycle rear wheel simulator repeatability results

Acceleration response	Strain response
Repeatability number = 97.80 %	Repeatability number = 98.15 %

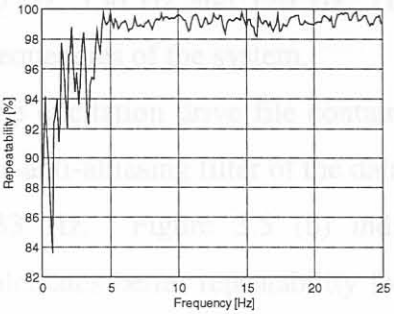
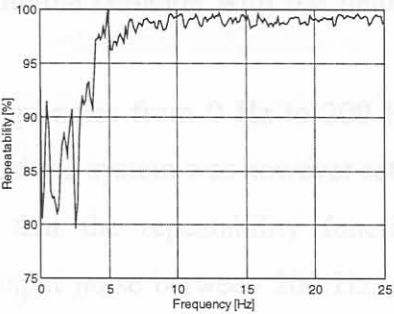
The repeatability results for the motorcycle rear wheel road simulator show the distinct differences between the characteristics of acceleration and strain responses. Accelerometers, and acceleration as such, exhibit poor sensitivity at low frequencies. Strain responses on the other hand show good low frequency response, with less sensitivity at increasing frequencies. Poor sensitivity gives rise to poor signal to noise ratios and subsequently poor repeatability.

3.1.4. Repeatability function application 4: Radiator test rig

Vibration tests were conducted on a vehicle radiator assembly. The test rig made use of a rigid mounting frame, installed vertically on a servo-hydraulic actuator. Mounting pins on the top and bottom radiator tanks fitted into doughnut shaped rubber mounts. These rubber mounts were fitted to the rigid mounting frame. Play between the mounting pins and the rubber mounts allowed some free movement of the radiator, both vertically and horizontally.

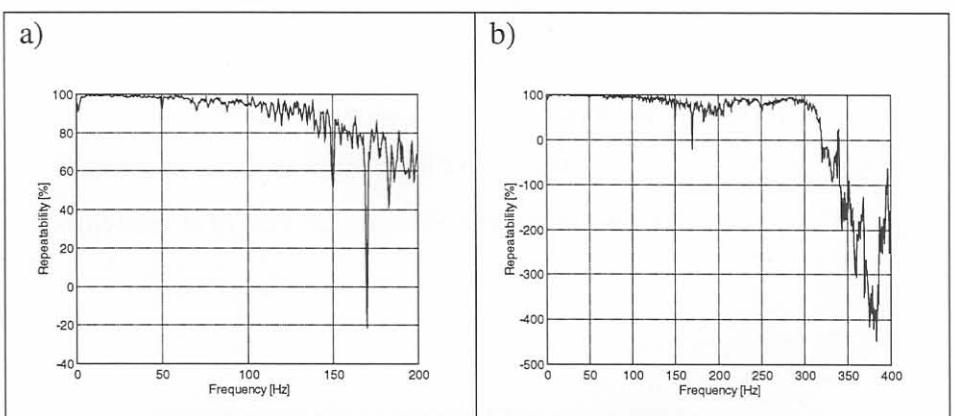
Acceleration responses were recorded on the base of the mounting frame, and on the top tank of the radiator. The repeatability of the base and top tank accelerations are compared in Table 3.3 for a simulation bandwidth of 0 Hz to 25 Hz.

Table 3.3 Radiator test rig repeatability results

Mounting base acceleration	Radiator top tank acceleration
	
Repeatability number = 97.76 %	Repeatability number = 96.95 %

The repeatability results are similar for both transducer locations. The repeatability numbers differ with only 0.81 percentage points.

A second frequency related repeatability test was conducted on the top tank accelerometer response. A 0 Hz to 200 Hz drive signal was used to excite the tests system. The results for this wide-band test are shown in Figure 3.5. Figure 3.5(a) shows the repeatability vs. frequency graph for the 0Hz to 200 Hz excitation bandwidth. Figure 3.5(b) is the same set of results, presented over a wider 0 Hz to 400 Hz frequency band.

**Figure 3.5 Radiator top tank repeatability, 0Hz – 200 Hz**

The repeatability of the radiator top tank acceleration response is relatively constant between 5 Hz and ± 60 Hz, except for a slight decline at 50 Hz (alternating current power supply). Globally, the

repeatability graphs decreases from frequencies above 100 Hz, which coincides with the frequency response of the hydraulic servo control valve. Some distinct minima are evident from the repeatability plot at 70 Hz, 150 Hz and 170 Hz. These minima coincide with the natural frequencies of the system.

The excitation drive file contained frequencies from 0 Hz to 200 Hz, the anti-aliasing filter of the data acquisition system was however set at 333 Hz. Figure 3.5 (b) indicates that the repeatability function calculates better repeatability for the input noise between 200 Hz and 333 Hz, than for large sections of the 0 Hz to 200 Hz signal.

- The validity of comparing PSD amplitudes to determine frequency related repeatability is questionable. The radiator test rig example showed better repeatability for frequencies above the test bandwidth (i.e. system noise), than for sections of the driven system response.
- Typical scalar repeatability numbers are in the region of 98% - 99.9%. The linear percentage scale is not sensitive enough to clearly show the effect of repeatability on simulation. A more sensitive parameter is needed to quantify test rig repeatability.

3.1.5. General discussion of repeatability test procedure and results

The scalar and frequency related repeatability functions defined in Section 3.1 provide the test engineer with some indication on the repeatability of the test system's input/output behaviour. These functions do however require further refinement, as both are not ideally suited for application in time domain modelling and simulation.

- Accurate frequency analysis, such as PSD calculations, requires long sections of time data. One of the drives behind time domain simulation is the capability of using short excitation data for model identification. The advantages of short identification signals would become irrelevant considering the lengthy sections of data needed to compute such a frequency related repeatability function. Further investigations into accurate frequency analysis using shorter sections of data could place a new perspective on a function of repeatability vs. excitation frequency.
- The validity of comparing PSD amplitudes to determine frequency related repeatability is questionable. The radiator test rig example showed better repeatability for frequencies above the test bandwidth (i.e. system noise), than for sections of the driven system response.
- Typical scalar repeatability numbers are in the region of 98% ~ 99.9%. The linear percentage scale is not sensitive enough to clearly show the effect of repeatability on simulation. A more sensitive parameter is needed to quantify test rig repeatability.

Figure 3.6: Spill spectra modeling

3.2. Split spectra modelling and simulation

The concept of split spectra time domain modelling was initially proposed to reduce the effect of resonant peaks in the system response on simulation results. The philosophy is to model the broad-spectrum behaviour of a system with two or more narrow bandwidth time domain models. The procedure is illustrated in Figure 3.6 for a two-way split of 0 ~ 80 Hz data.

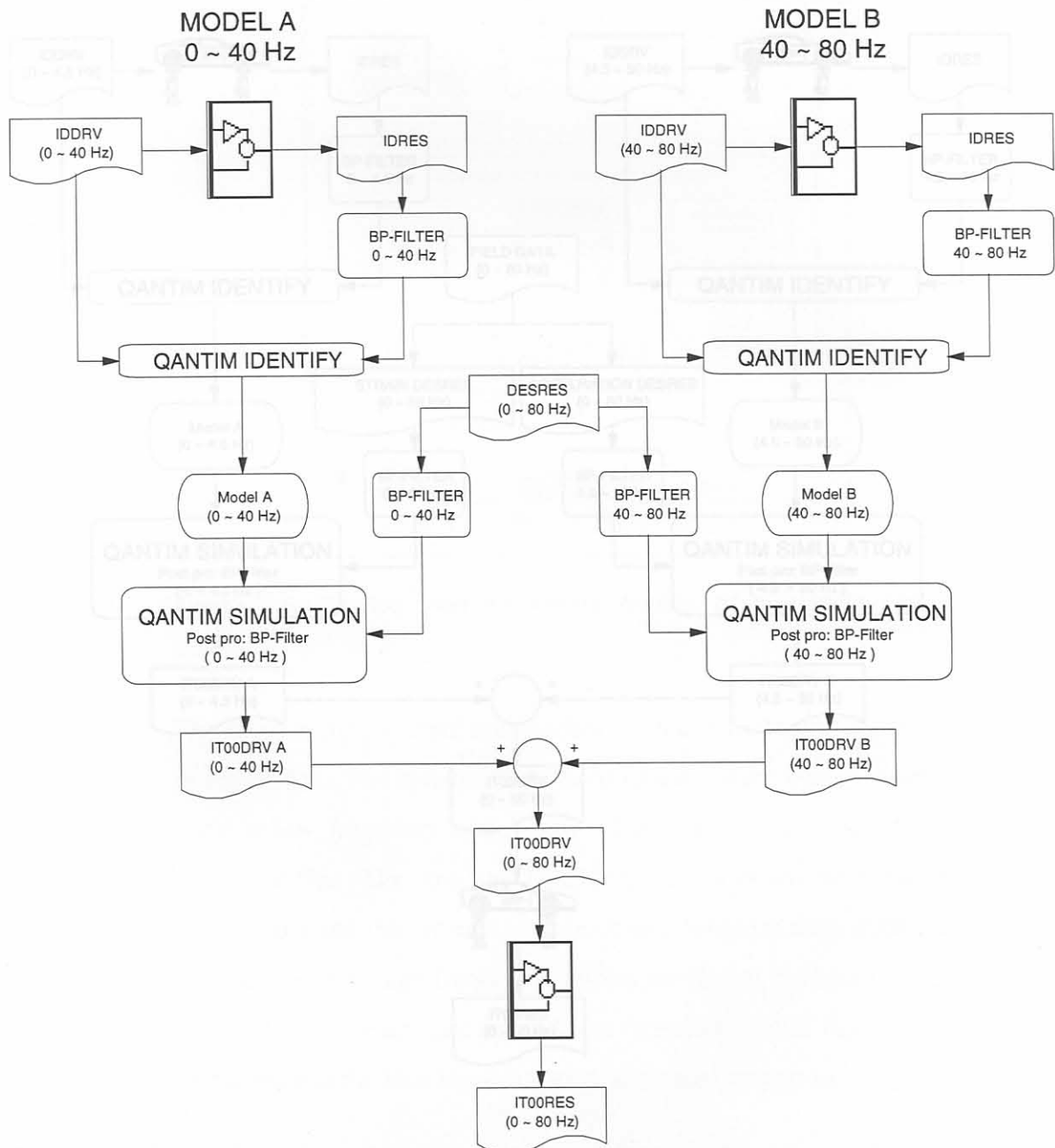


Figure 3.6: Split spectra modelling

The concept of split spectra modelling was further extended by using separate transducers for different frequency bandwidths. This was done to optimally utilise each transducer frequency response. A typical example being the measurement of wheel movements of a motorcycle as presented in Section 3.2.2. A flow diagram illustrating split spectra modelling and simulation with separate transducers is shown in Figure 3.7.

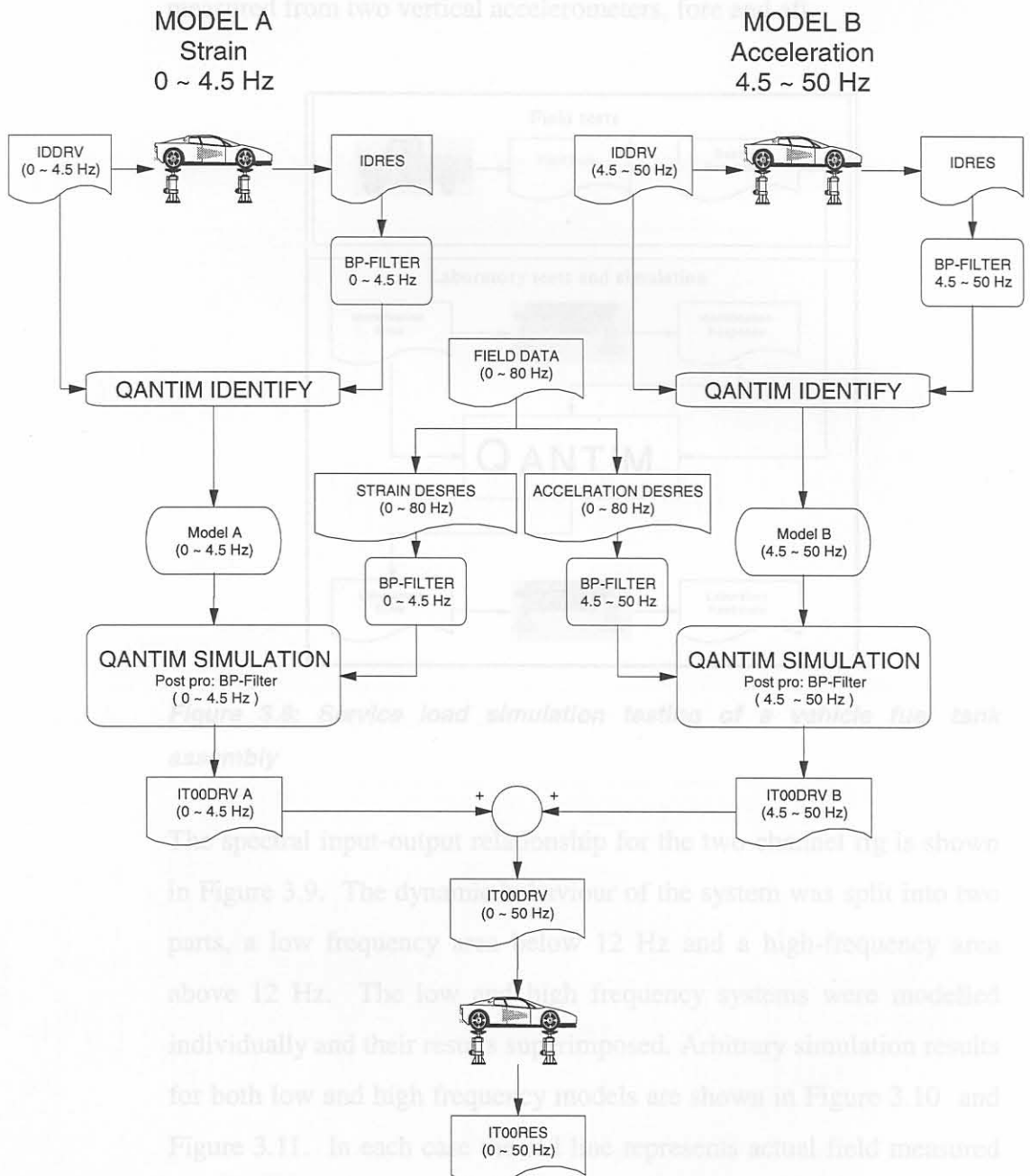


Figure 3.7 Split spectra modelling, using separate transducers

3.2.1. Application of split spectra simulation on a fuel tank test rig

A simulation test on a delivery vehicle fuel tank assembly is discussed as an example of the implementation of split spectra modelling. The basic steps of service load simulation testing, as introduced in chapter 1.3 is again presented in Figure 3.8 for the fuel tank test rig [50]. The fuel tank assembly was mounted on two vertical actuators, and response measured from two vertical accelerometers, fore and aft.

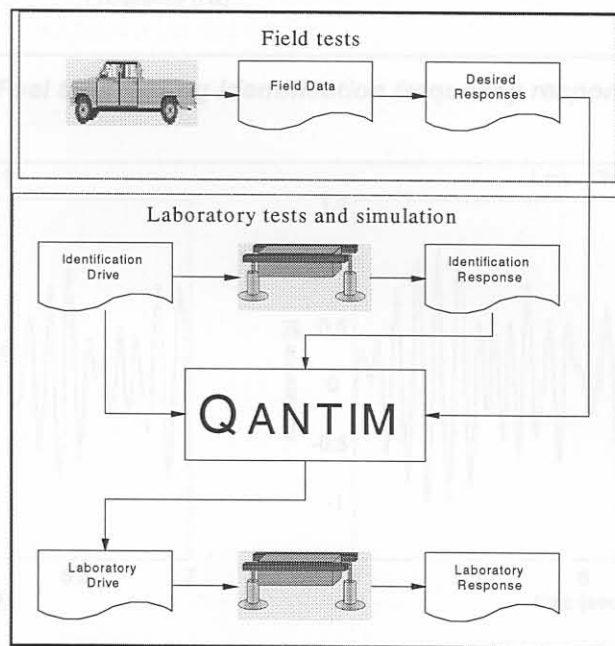


Figure 3.8: Service load simulation testing of a vehicle fuel tank assembly

The spectral input-output relationship for the two-channel rig is shown in Figure 3.9. The dynamic behaviour of the system was split into two parts, a low frequency area below 12 Hz and a high-frequency area above 12 Hz. The low and high frequency systems were modelled individually and their results superimposed. Arbitrary simulation results for both low and high frequency models are shown in Figure 3.10 and Figure 3.11. In each case the red line represents actual field measured responses and the blue line laboratory simulated responses.

Figure 3.11: High frequency simulation results

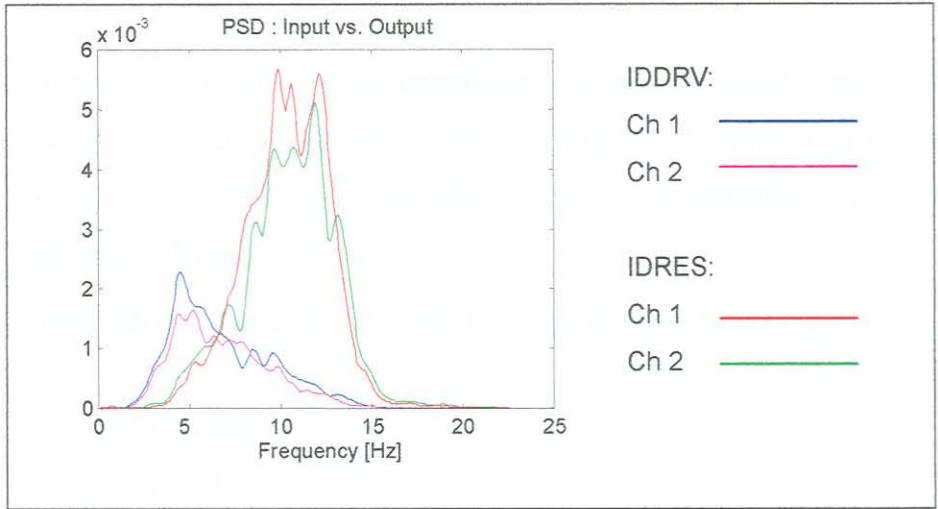


Figure 3.9: Fuel tank test rig identification frequency response

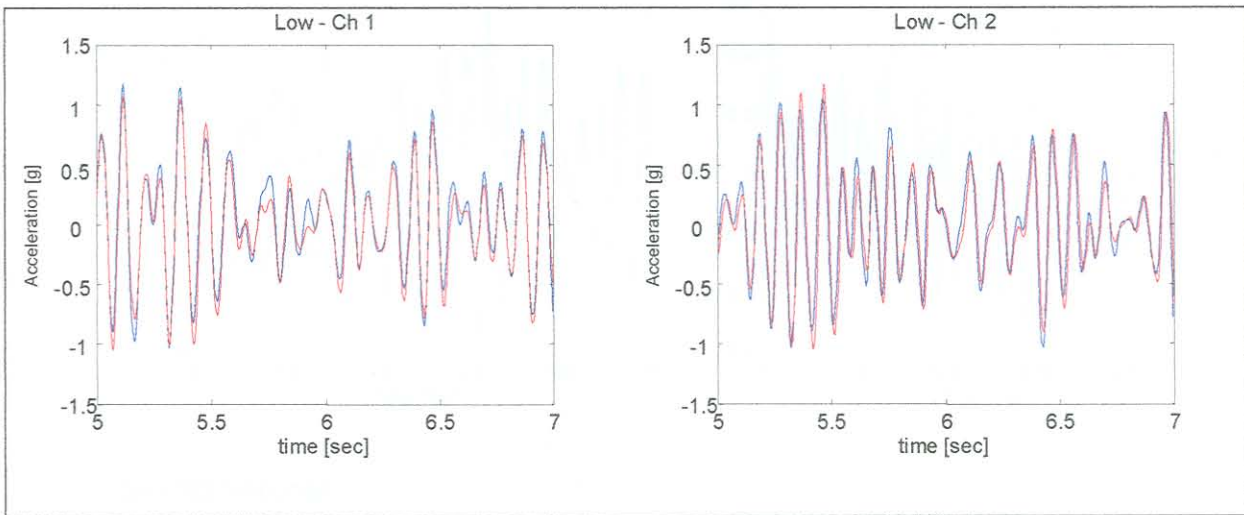


Figure 3.10: Low frequency simulation results

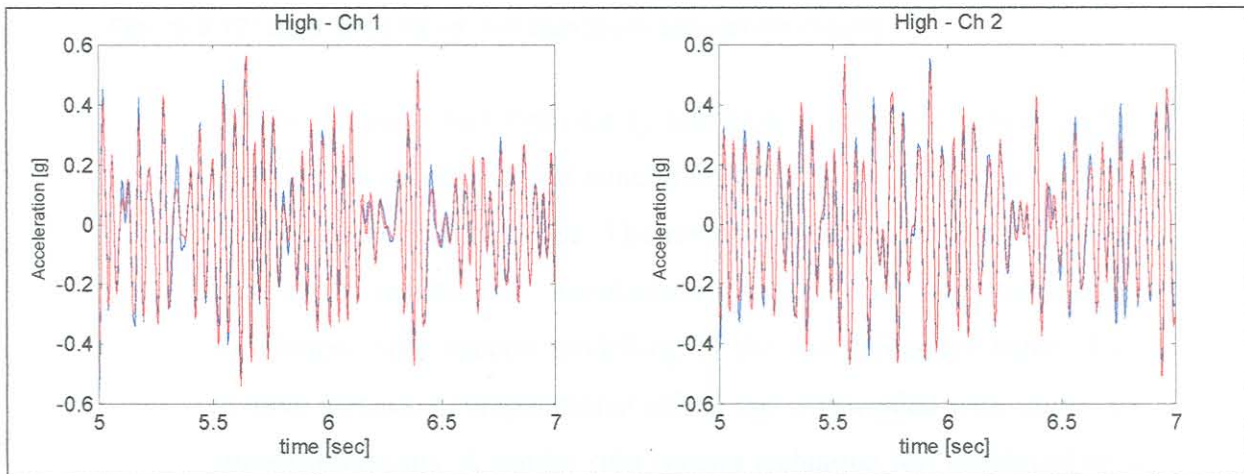


Figure 3.11: High frequency simulation results

Comparative results for the combined split spectra models and a full spectrum model are shown in Table 3.4 Figure 3.12 The error values (see Section 5.7) for each channel quantifies the advantages of split spectra modelling.

Table 3.4: QanTiM error values for split and full spectra simulation

	Channel 1	Channel 2
Full spectra model	46	46
Combined split spectra model	20	19

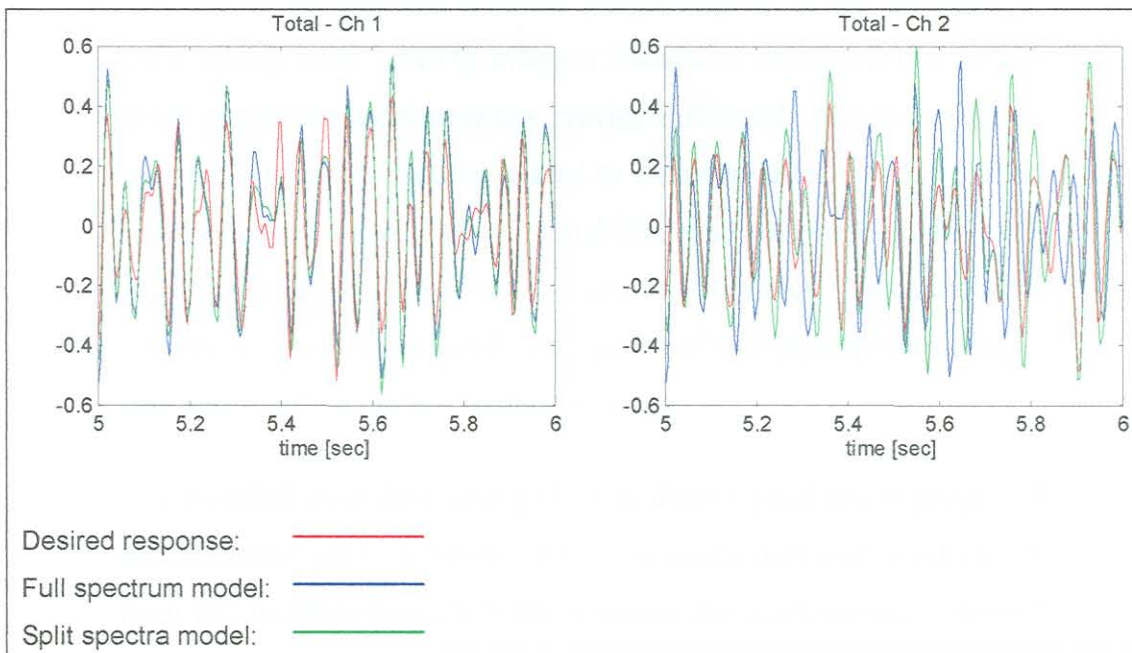


Figure 3.12: Split spectra vs. full spectrum simulation results

The two channel fuel tank test system clearly exhibits the potential of split spectra modelling and simulation to improve results for systems with resonant field response. The resonant peak within the simulation bandwidth resulted in unsatisfactory modelling and subsequent simulation. Split spectra modelling of the two frequency bands does involve increased computational effort, but is rewarded with improved simulation results. A similar split spectra technique was employed on a three-axis heavy vehicle chassis simulator with equally favourable results. [45]

3.2.2. Application of split spectra simulation on motorcycle simulator

A simulation example using multiple transducer split-spectra modelling is presented for the rear suspension of a motorcycle on a single axis road simulator. The motorcycle rear suspension road simulator was presented in Section 3.1.3. Typical simulation of field response data is normally conducted using a single remote parameter transducer for each simulation channel. In the case of vehicle simulations, spindle mounted accelerometers, or strain gauges applied to the coil springs, are normally used. Due to inherent transducer characteristics neither strain gauges nor accelerometers provide sufficiently sensitive response over the typical bandwidths related to automotive testing. The small strain amplitudes associated with high frequency responses make strain gauges less sensitive with an increase in frequency. Accelerometer sensitivity, on the other hand, is proportional to frequency, resulting in poor sensitivity in the low frequency ranges.

The recorded field data clearly showed these typical strain gauge and accelerometer characteristics. The strain gauge data contained energy from DC to approximately 8 Hz, whereas the accelerometers showed energy from approximately 8 Hz to 30 Hz.

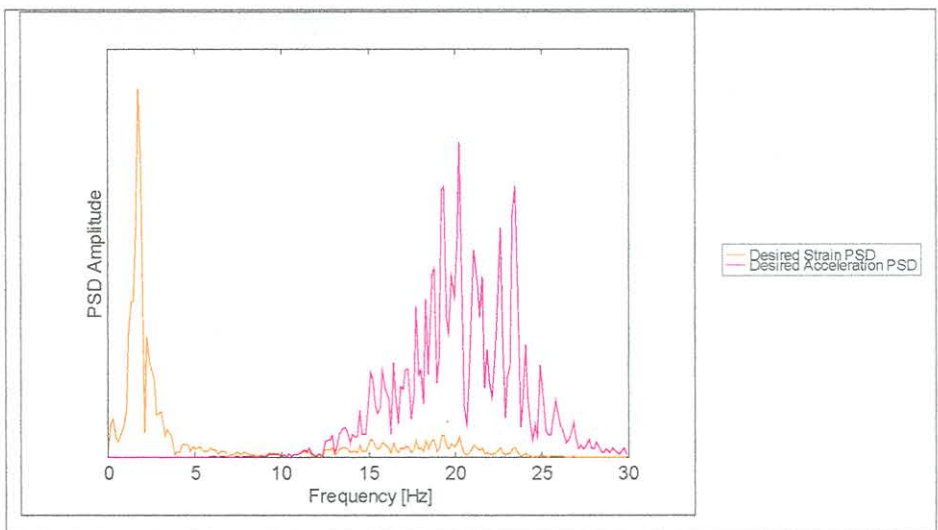


Figure 3.13 Motorcycle rear suspension desired response PSD

From the spectral plots in Figure 3.13 it was decided to split the responses at 8 Hz. The upper limit for simulation was chosen at 30Hz. Subsequently the strain responses were low-pass filtered at 8 Hz and the acceleration responses band-pass filtered between 8 Hz and 30Hz. The simulation results for the multiple transducer split spectra procedure are presented in Figure 3.14. The split spectra results are subsequently compared to results obtained with broad spectrum, single transducer simulations. In order to compare the effect of the modelling techniques, only the linear solution results are presented i.e. no iterations are performed subsequent to simulation.

Figure 3.15, Figure 3.16 and Figure 3.17 compare the simulation results of the conventional single transducer, broad-spectrum QanTiM simulations, with that of the split spectra, multiple transducer technique.

- The broad spectrum strain simulation results in a generally good simulation of both strain and acceleration response. The strain simulation does however produce too large amplitudes at low frequencies, and small amplitudes at higher frequencies.
- The broad-spectrum acceleration simulation provides good high frequency results, but poor simulation of the low frequency strains.
- The split spectra model results in improved simulation over the full simulation bandwidth.



Figure 3.14 Multiple transducer split spectra simulation results

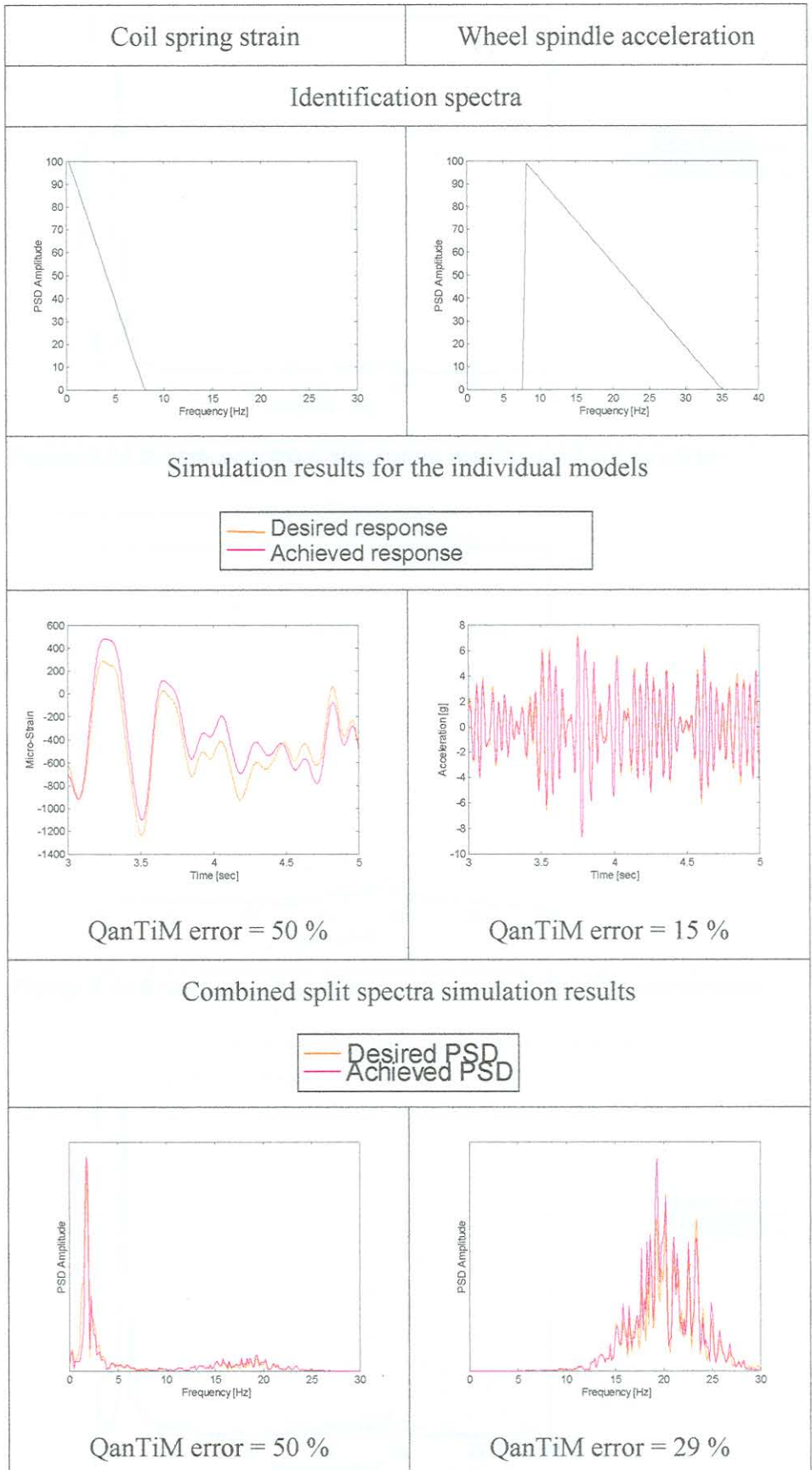


Figure 3.14 Multiple transducer split spectra simulation results

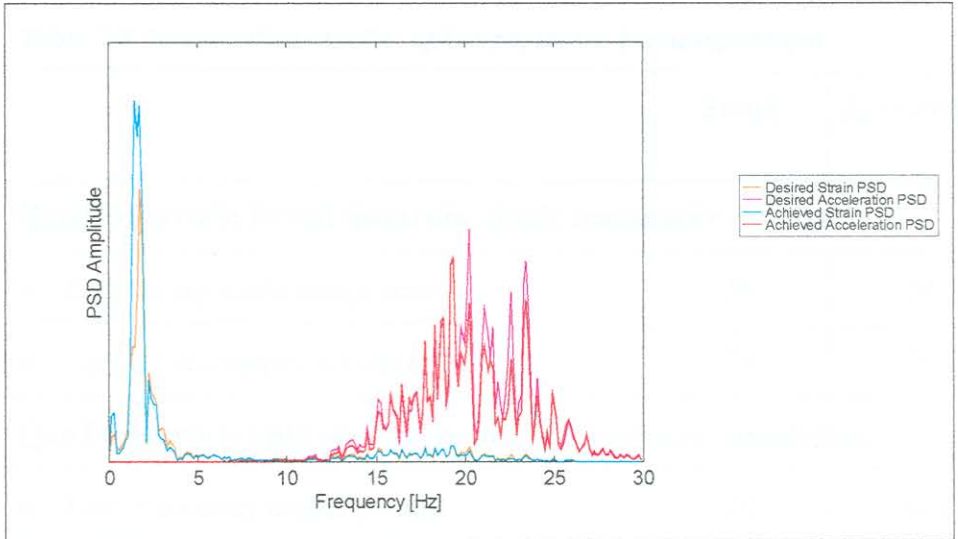


Figure 3.15 Broad- spectrum simulation results: Coil spring strain

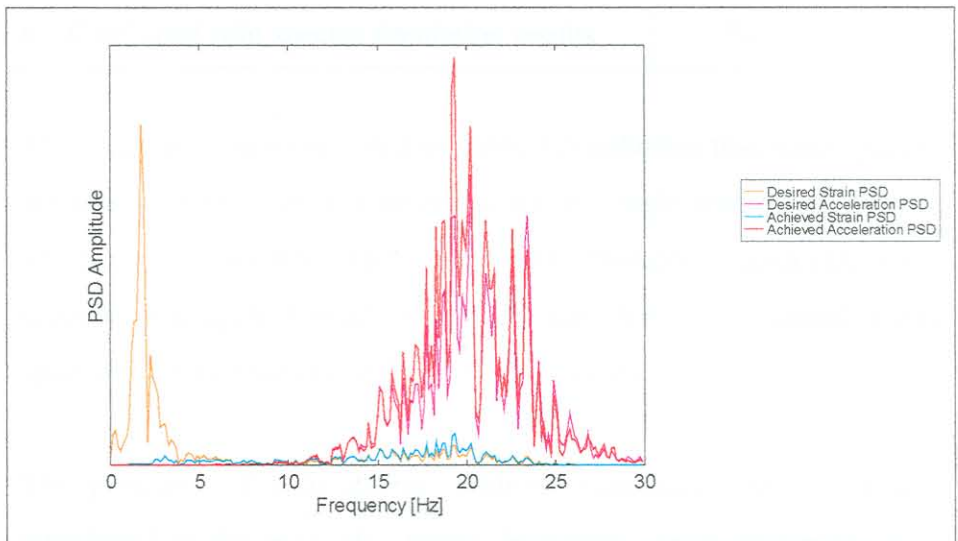


Figure 3.16 Broad- spectrum simulation results: Spindle acceleration

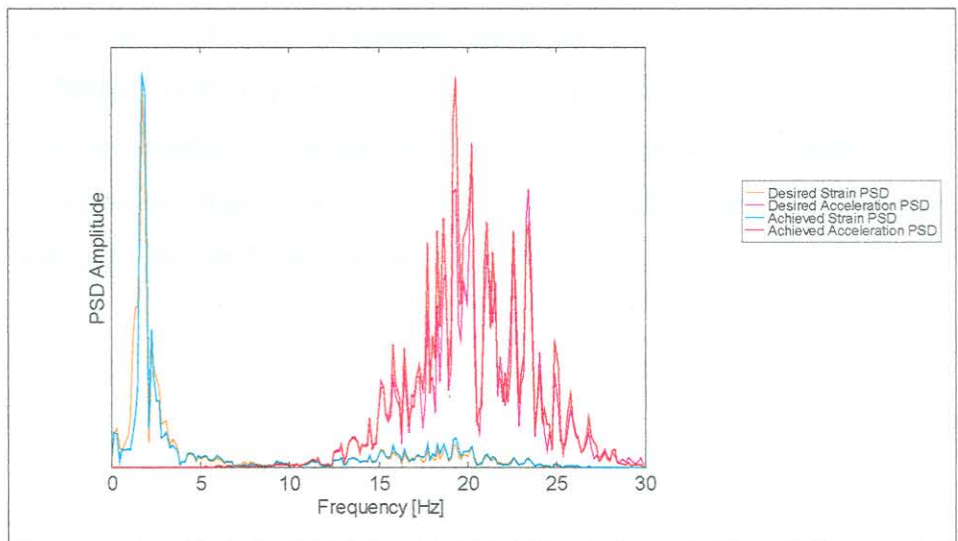


Figure 3.17 Split spectra simulation results

Table 3.5 Comparative results: split-spectra vs. broad-spectrum

	Strain	Acceleration
QanTiM errors: Broad spectrum, single transducer simulation		
• Coil spring strain gauge simulation	56	51
• Spindle accelerometer simulation	78	31
QanTiM errors: Split spectra, multiple transducer simulation		
• Low frequency model (strain)	50	N/A
• High frequency model (acceleration)	N/A	15
• Combined split spectra simulation results	50	29

The result summary presented in Table 3.5 indicates that strain gauges are more effective than accelerometers as single transducer, remote simulation parameters. More important, multiple transducer, split-spectra simulation proved more accurate than conventional broad spectrum, single transducer QanTiM simulations.

The principle of split-spectra, multiple transducer simulation was introduced at the hand of a relatively simple, single-axis application example. Vehicle simulation tests on four post road simulators benefit from the extended frequency bandwidths achievable with this technique. Low frequency, high amplitude response, such as body twist, can be accurately reproduced using this split spectra technique. The accurate simulation of such low frequency responses may have a marked effect on fatigue predictions.

3.3. Optimal excitation characteristics

The PSD function from which the identification drive signals are generated can have notable effect on the simulation outcome. Frequency domain simulation systems usually make use of a $1/f^n$ PSD function to create identification drive signals. The $1/f$ PSD, as shown in Figure 3.18a, is normally representative of a servo hydraulic actuator's dynamic capabilities. A similar approach is generally followed for time domain identification, although a triangular PSD function is found to give better results [15], [13], [24].

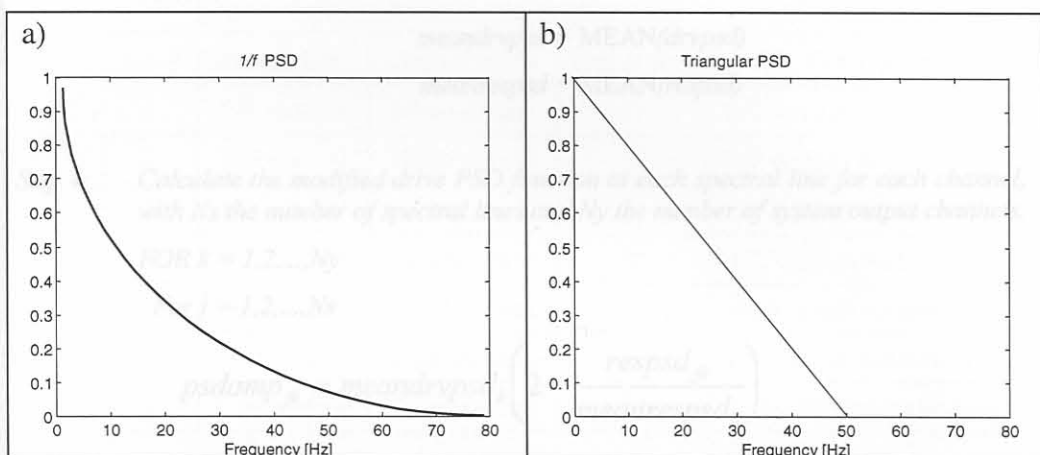


Figure 3.18: $1/f$ and triangular PSD functions for identification drive signals.

The $1/f^n$ and triangular PSD functions proved limited for systems with intricate dynamic behaviour [17]. A method for finding an optimised PSD function is needed, especially for multi-axial test rigs. Based on the work by Barnard [2], the author devised a simple method of anti-resonant excitation to create an identification drive signal well suited to a specific test rig. This purely intuitive method limits the excitation PSD function in the areas of system resonance. The procedure for finding a set of rig specific identification drive PSD's is described briefly in Algorithm 3.1 and an application example is given. The example in Figure 3.19 shows the sine sweep drive and response PSD functions as well as the modified rig specific PSD function for a single axis test rig. A detailed application example is presented in Section 3.3.1 for a seven-channel fuel tank test rig.

Algorithm 3.1: Rig specific identification PSD's

Step 1: Excite all channels of the rig with a low amplitude linear sine sweep within the typical frequency bandwidth of the system. Simultaneously record the responses from the relevant transducers.

Step 2: For each channel calculate the PSD functions of both the drive and response signals so that:

$$drvpsd = \text{PSD}(\text{sweepdrive})$$

$$respsd = \text{PSD}(\text{sweepres})$$

Where *drvpsd* and *respsd* are matrices with row entries containing the PSD amplitudes at each specified spectral line for all the input and output channels of the system.

Step 3: Calculate the mean value of the PSD amplitudes in *drvpsd* and *respsd* for each channel:

$$\text{meandrvpsd} = \text{MEAN}(\text{drvpsd})$$

$$\text{meanrespsd} = \text{MEAN}(\text{respsd})$$

Step 4: Calculate the modified drive PSD function at each spectral line for each channel, with *Ns* the number of spectral lines and *Ny* the number of system output channels.

FOR $k = 1, 2, \dots, Ny$

For $j = 1, 2, \dots, Ns$

$$\text{psdamp}_{jk} = \text{meandrvpsd}_k \left(2 - \frac{\text{respsd}_{jk}}{\text{meanrespsd}_k} \right)$$

Step 5: Create a random identification drive signal using the modified PSD function.

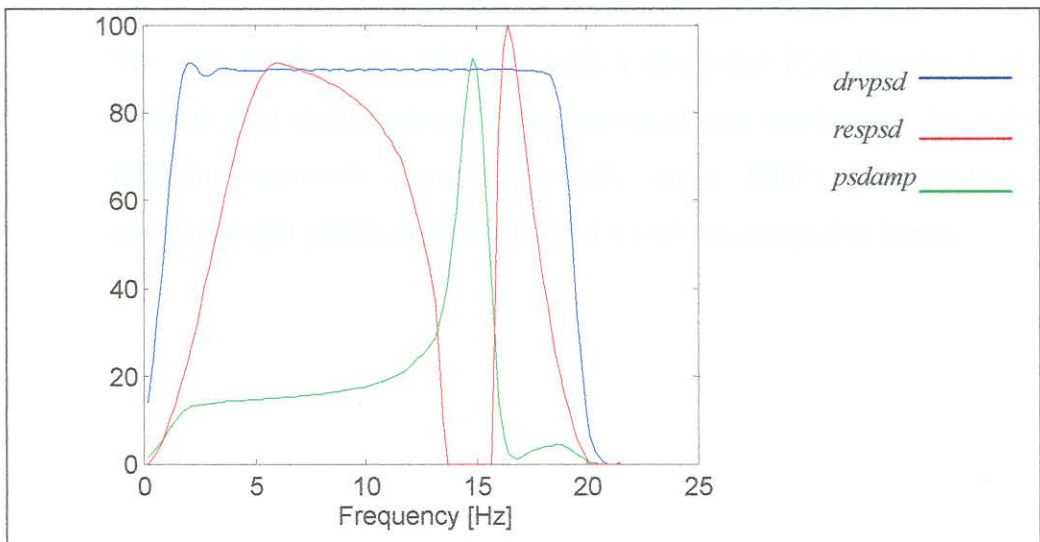


Figure 3.19: Rig specific PSD calculation

3.3.1. Application on a seven channel fuel tank test rig

QanTiM was used to drive a MTS 498 seven-channel full chassis fuel tank test rig [17] (courtesy of Ford motor co. Dearborn). The inputs to the rig consisted of vertical displacements at the four corners, as well as two lateral displacements, and a longitudinal displacement. The responses were measured from accelerometers mounted near the actuator connecting points.

Table 3.6: Test rig summary

Ch #	Test rig drive characteristics			Model response
	Description	Control mode	Full scale	Description
1	L/F vertical	Displacement	3"	L/F vertical acceleration
2	R/F vertical	Displacement	3"	R/F vertical acceleration
3	L/R vertical	Displacement	3"	L/R vertical acceleration
4	R/R vertical	Displacement	3"	R/R vertical acceleration
5	Front lateral	Displacement	3"	Front lateral acceleration
6	Rear lateral	Displacement	3"	Rear lateral acceleration
7	Longitudinal	Displacement	3"	Longitudinal acceleration

Despite the rig's apparent simplicity, numerous modelling iterations were performed without any success. Typical triangular and $1/f$ drive PSD's with various amplitudes were used, all with equally poor results. The best results were achieved with a triangular PSD ranging from 1~40Hz used along with relatively high excitation amplitudes. A totally different approach using rig-specific drive PSD's proved more successful and produced modelling errors within acceptable limits.

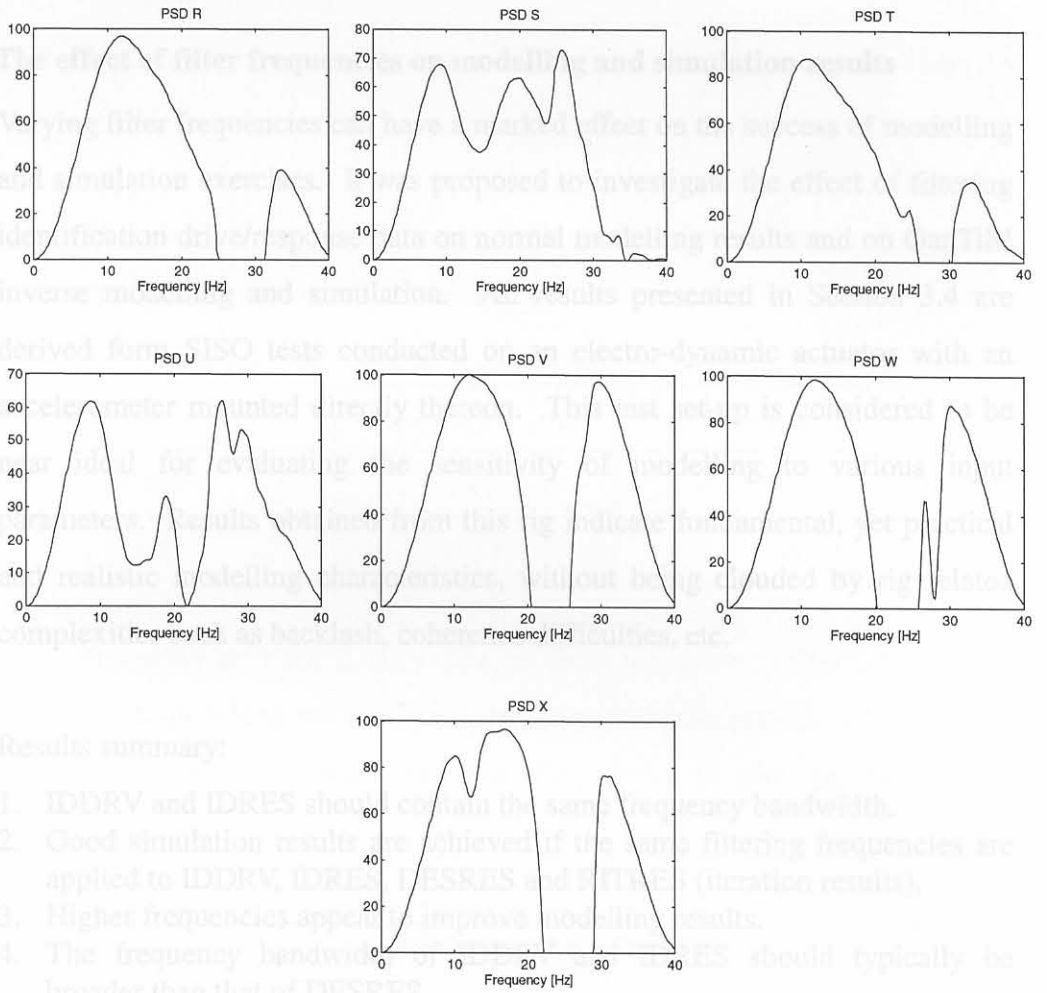
In order to gain some knowledge of the rig characteristics, a 0~40Hz linear, small amplitude, (0.015") sine sweep was driven through the four vertical actuators. The PSD's of the sweep input / output data were used to create a drive PSD that would minimise energy in the rig's regions of resonance. This proved effective for the vertical channels and the process was repeated for all seven actuators. The result was a set of seven unique PSD's from which the identification drive signals were generated. The modelling results improved drastically and showed some potential for rig-specific PSD's. The models created with the rig-specific PSD's seemed inherently stable, as is shown in a typical model order selection plot. (The concept of QanTiM model orders are discussed in Section 4.2) The modelling error tended to decrease with order without signs of instability; this seemed to be the case for all channels.

Table 3.7: MISO rig specific modelling results

Ch	Description	IDDRV Parameters		GPREPRO Filter cut-off frequencies		Modelling results	
		PSD	Amp	Low	High	order	error
1	L/F vertical	R	1"	1 Hz.	40 Hz.	4	20
2	R/F vertical	S	1"	1 Hz.	40 Hz.	9	22
3	L/R vertical	T	1"	1 Hz.	40 Hz.	6	19
4	R/R vertical	U	1"	1 Hz.	40 Hz.	7	29
5	Front lateral	V	0.2"	1 Hz.	40 Hz.	5	23
6	Rear lateral	W	0.2"	1 Hz.	40 Hz.	7	19
7	Longitudinal	X	0.2"	1 Hz.	40 Hz.	6	37



Figure 3.21: Model error vs. order for channel 1



Results summary:

1. IDDRV and IDRES show good results within the same frequency bandwidth.
2. Good simulation results are achieved if the same filtering frequencies are applied to IDDRV, IDRI, IDRESSES and FITRES (iteration results).
3. Higher frequencies appear to improve modelling results.
4. The frequency bandwidth of the simulation should typically be broader than that of DESRES.
5. Models identified from broad spectrum data showed good iteration results.

Figure 3.20: Rig specific PSD functions

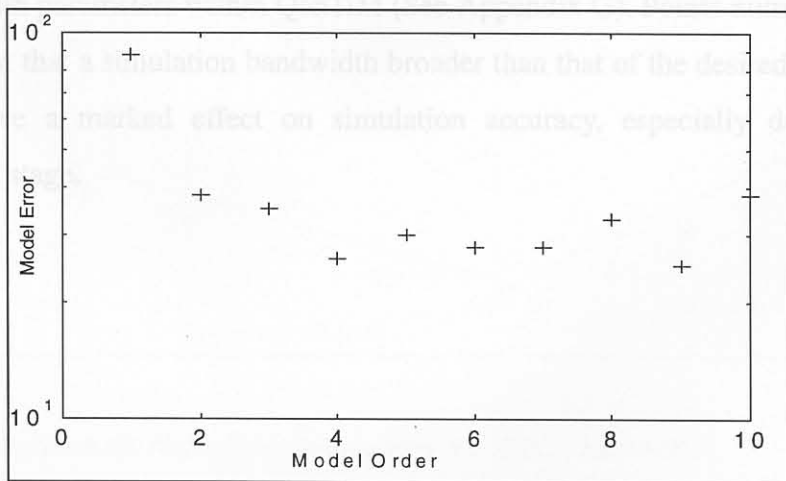


Figure 3.21: Model error vs. order for channel 1

3.4.1. Normal modelling

3.4. The effect of filter frequencies on modelling and simulation results

Varying filter frequencies can have a marked effect on the success of modelling and simulation exercises. It was proposed to investigate the effect of filtering identification drive/response data on normal modelling results and on QanTiM inverse modelling and simulation. All results presented in Section 3.4 are derived from SISO tests conducted on an electro-dynamic actuator with an accelerometer mounted directly thereon. This test set-up is considered to be near ideal for evaluating the sensitivity of modelling to various input parameters. Results obtained from this rig indicate fundamental, yet practical and realistic modelling characteristics, without being clouded by rig related complexities such as backlash, coherence difficulties, etc.

Results summary:

1. IDDRV and IDRES should contain the same frequency bandwidth.
2. Good simulation results are achieved if the same filtering frequencies are applied to IDDRV, IDRES, DESRES and RITRES (iteration results).
3. Higher frequencies appear to improve modelling results.
4. The frequency bandwidth of IDDRV and IDRES should typically be broader than that of DESRES.
5. Models identified from broad spectrum data showed good iteration characteristics

Points number 1 and 2 led to the implementation of general simulation bandwidth parameters within QanTiM (See Appendix G). Points number 4 and 5 suggest that a simulation bandwidth broader than that of the desired response may have a marked effect on simulation accuracy, especially during the iteration stage.

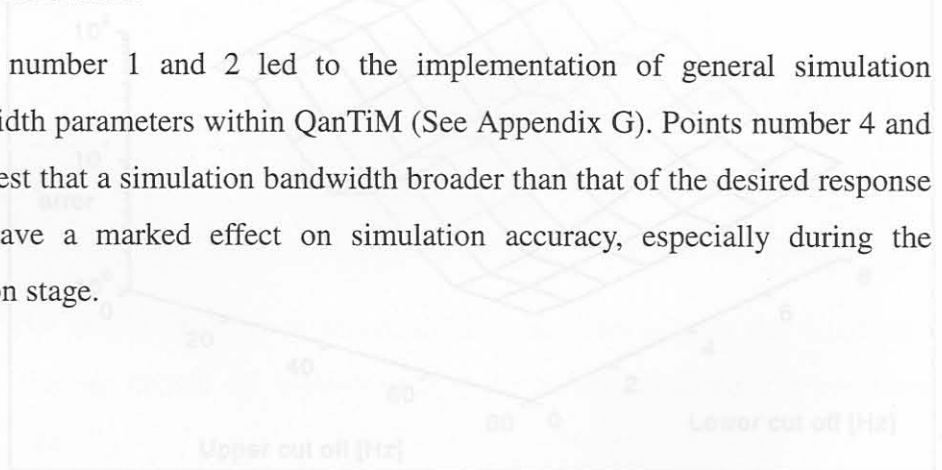


Figure 3.22: Normal modelling error vs. IDRES bandwidth

3.4.1. Normal modelling

Two sets of filtering exercises were conducted using normal QanTiM (ARX)-models. Firstly models were calculated for a system excited with a broad-spectrum random signal and band filtered responses. Thereafter both identification drive and response signals were band pass filtered prior to modelling.

	lower cut off [Hz]	Upper cut off [Hz]
IDDRV	0	80
IDRES	0 ~ 8	16 ~ 80

Filtering only the IDRES data, as presently done in QanTiM, showed high modelling errors as the signal bandwidth decreased. This is shown in Figure 3.22 where the modelling error is plot against IDRES bandwidth.

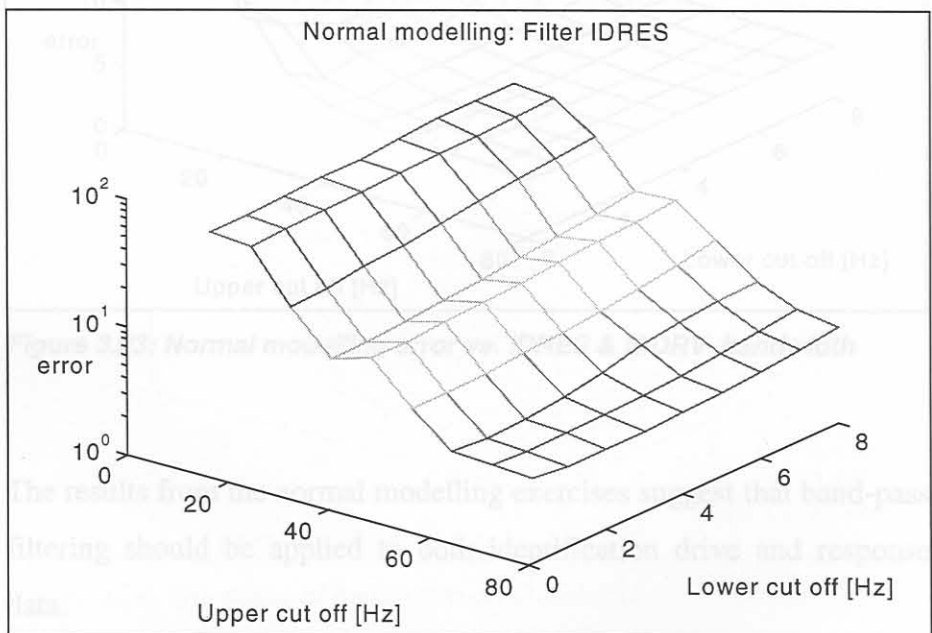


Figure 3.22: Normal modelling error vs. IDRES bandwidth

Using a band-pass filter on both IDDRV and IDRES prior to modelling greatly improved results. Modelling errors were generally reduced by a factor ten and showed good results for all frequency bandwidths wider than 20 Hz.

	lower cut off frequency [Hz]	Upper cut off frequency [Hz]
IDDRV	0 ~ 8	16 ~ 80
IDRES	0 ~ 8	16 ~ 80

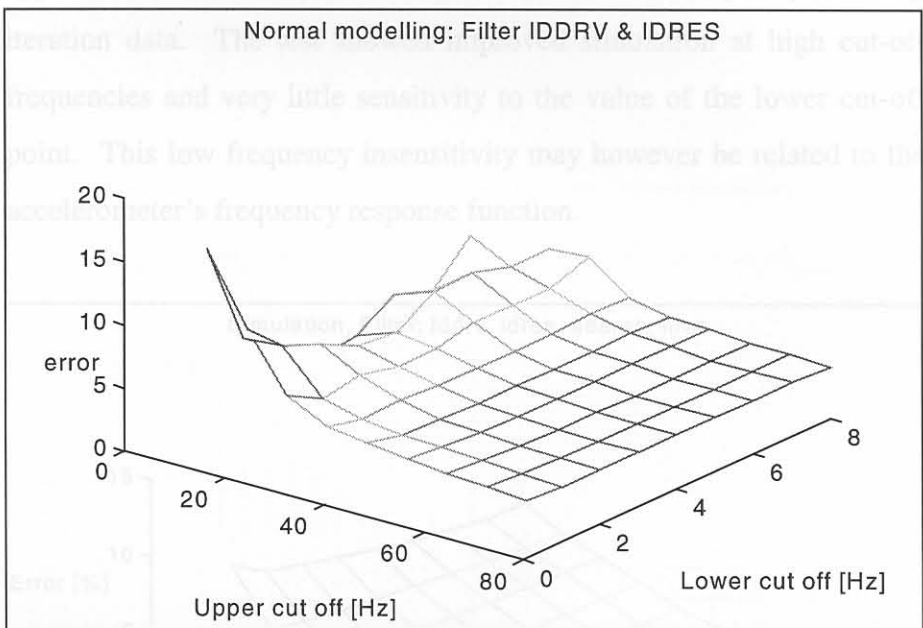


Figure 3.23: Normal modelling error vs. IDRES & IDDRV bandwidth

The results from the normal modelling exercises suggest that band-pass filtering should be applied to both identification drive and response data.

3.4.2. The effect of bandwidth on simulation

3.4.3. Tests were conducted to investigate the effects of modelling bandwidths on simulation results. The tests were conducted using desired response data recorded from the electro-dynamic test system while driving with either a 0 ~ 50 Hz or a 0 ~ 80 Hz random drive.

The results from the normal modelling exercise suggested that band-pass filtering should be applied to both identification drive and response data prior to modelling. This concept was further investigated for inverse QanTiM type models. The same band-pass criteria were applied to identification data, desired response data and post-processing iteration data. The test showed improved simulation at high cut-off frequencies and very little sensitivity to the value of the lower cut-off point. This low frequency insensitivity may however be related to the accelerometer's frequency response function.

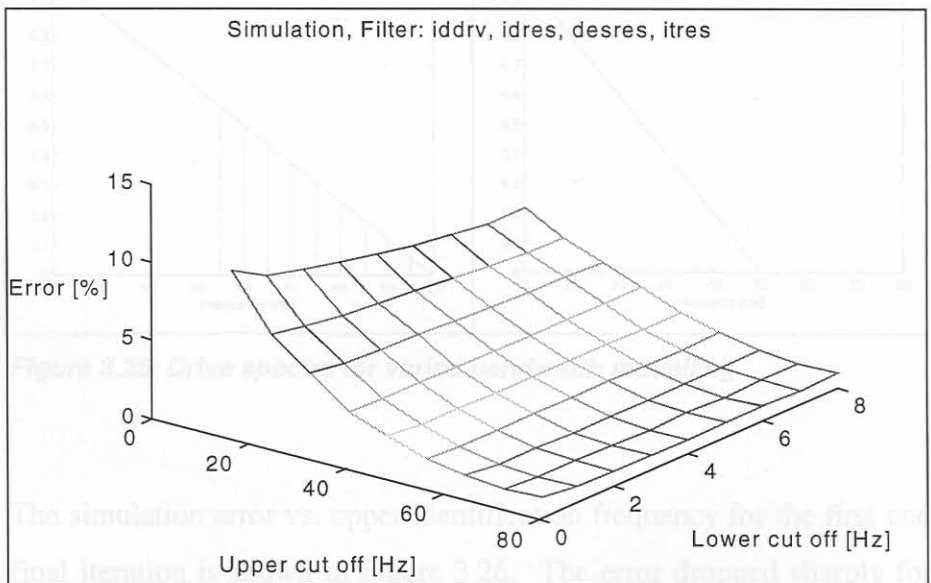


Figure 3.24: The effect of bandwidth on simulation

The simulation error vs. upper cut-off frequency for the first and final iteration is shown in Figure 3.26. The error decreased sharply for the first iteration and then remained stable up to 80 Hz (which returned the most accurate results after 4 iterations). Simulations using models identified with sub 50 Hz data tended to diverge during iteration, whereas the broader bandwidth models converged to a small error value (Figure 3.27).

3.4.3. Wide spectrum simulation

A series of tests were conducted to investigate the effect of identification bandwidth on simulation of a fixed desired response signal. Identification drive/response data was generated using a triangular full spectrum (0~80 Hz) PSD. Subsequently ten narrower bandwidth signals were generated by low-pass filtering according to Figure 3.25a. The desired response data was recorded from the system driven with the 0~50 Hz triangular PSD drive in Figure 3.25b. Prior to modelling a 2 Hz high-pass filter was used to compensate for low accelerometer sensitivity in the low frequency regions. No post-processing filtering operations were performed on the iteration response data

Figure 3.25: Simulation errors for iteration 0 and iteration 4

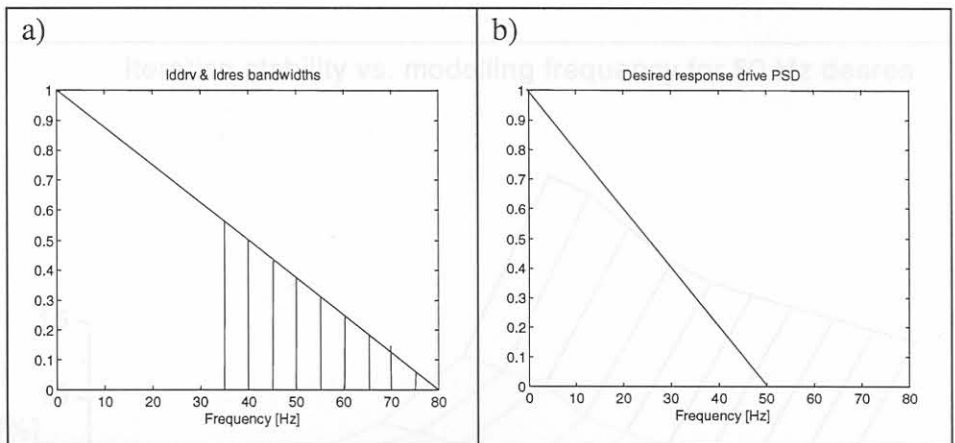


Figure 3.25: Drive spectra for varied bandwidth modelling

The simulation error vs. upper identification frequency for the first and final iteration is shown in Figure 3.26. The error dropped sharply for identification frequencies above 50 Hz, and remained stable up to 80 Hz (which returned the most accurate results after 4 iterations). Simulations using models identified with sub 50 Hz data tended to diverge during iteration, whereas the broader bandwidth models converged to a small error value.(Figure 3.27).

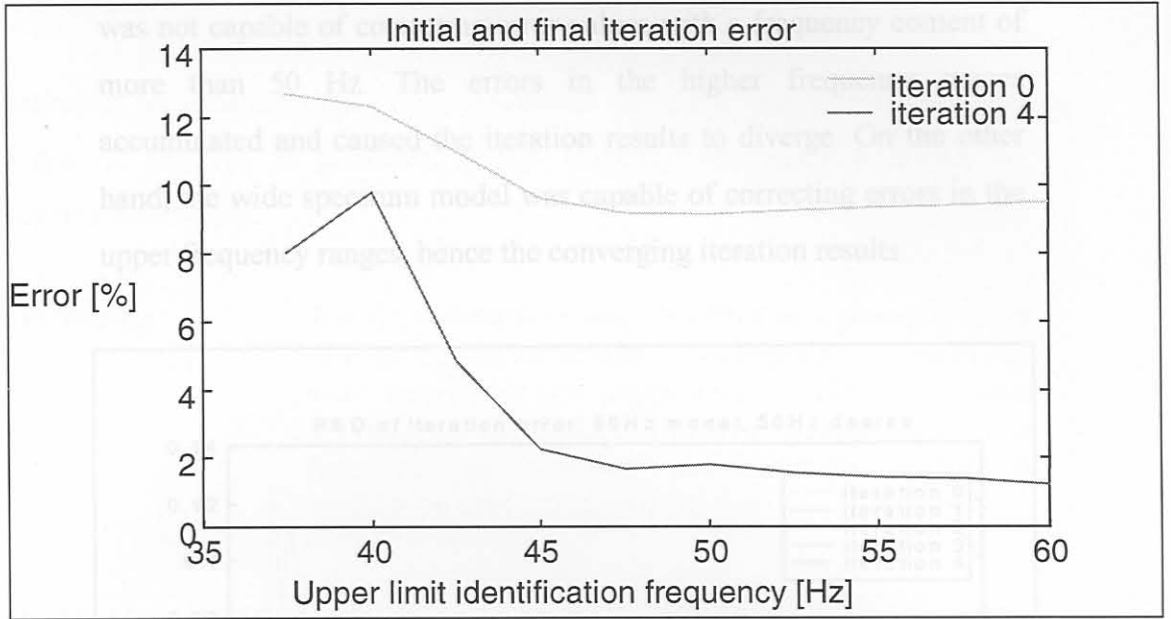


Figure 3.26: Simulation errors for iteration 0 and iteration 4

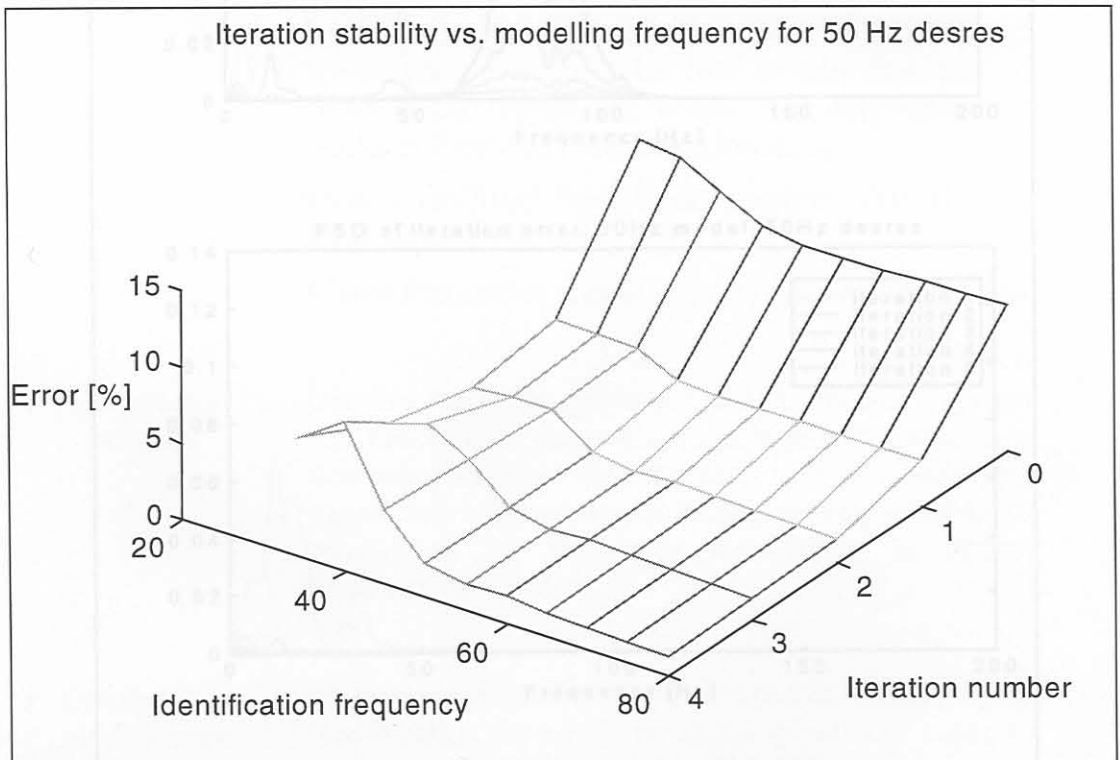


Figure 3.27: Iteration errors for various ID upper frequencies

PSD's of the iteration error signals are shown in Figure 3.28 for a 0 ~ 50 Hz model and a 0 ~ 80 Hz model. The narrower bandwidth model was not capable of correcting error values with a frequency content of more than 50 Hz. The errors in the higher frequency ranges accumulated and caused the iteration results to diverge. On the other hand, the wide spectrum model was capable of correcting errors in the upper frequency ranges, hence the converging iteration results.

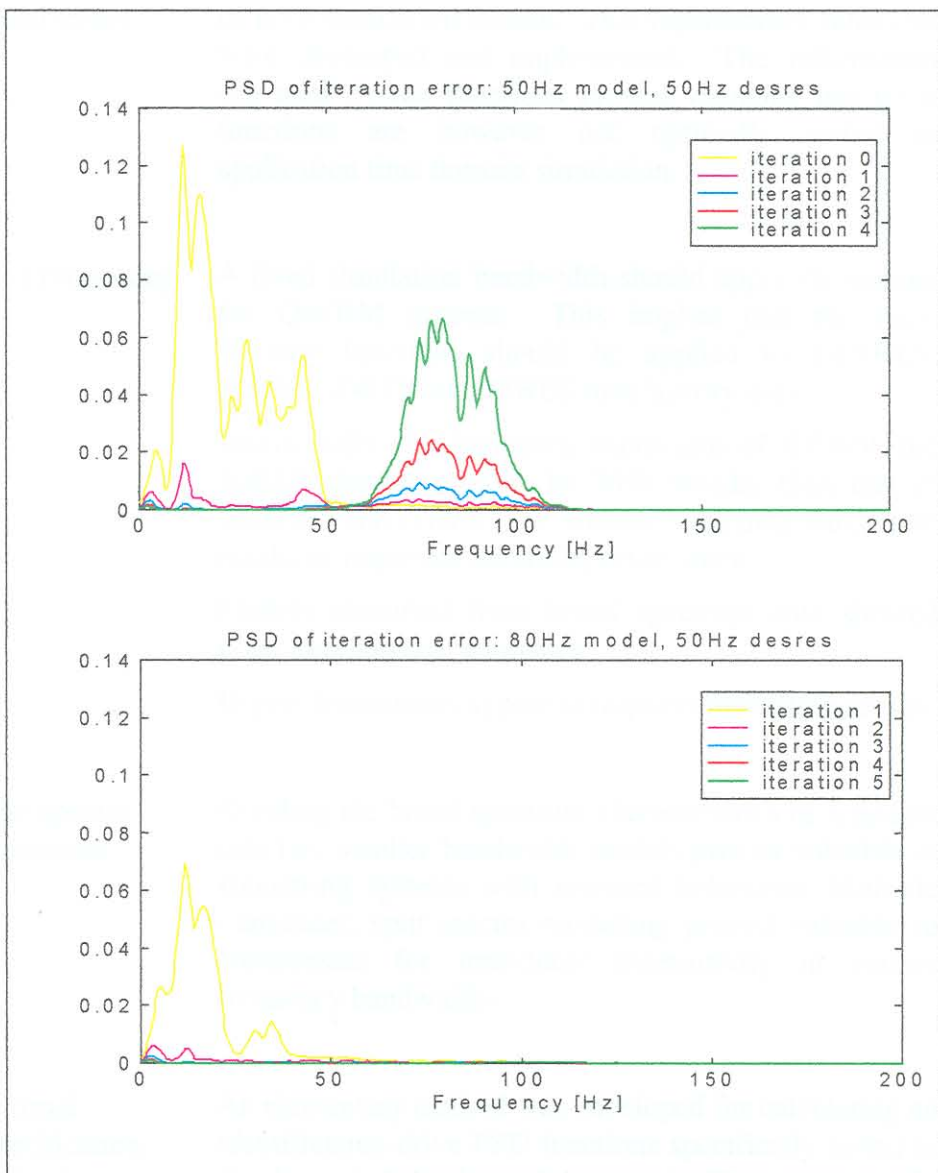


Figure 3.28: Iteration error frequency content

3.5. Conclusion and recommendations for further research - Part I

Valuable information concerning simulation accuracy was gained from the empirical research as presented in this chapter. The research results are summarised below.

- **Test rig repeatability** Test rig repeatability was identified as a potential cause of poor simulation results. Two repeatability functions were developed and implemented. The information provided by the functions proved valuable, but these functions are however not optimally suited to application time domain simulation.
- **Data processing** A fixed simulation bandwidth should apply throughout the QanTiM process. This implies that the same filtering functions should be applied to DESRES, IDDRV, IDRES, and ITRES time history data.

Additionally, the frequency bandwidth of IDDRV and IDRES should typically be 20% broader than that of DESRES and ITRES. The broader modelling bandwidth results in improved iteration performance.

Models identified from broad spectrum data showed good iteration characteristics

Higher frequencies appear to improve modelling results.
- **Split spectra simulation** Dividing the broad-spectrum characteristics of a system into two smaller bandwidth models proved valuable in simulating systems with resonant behaviour. Multiple transducer, split-spectra modelling proved valuable to compensate for transducer insensitivity in certain frequency bandwidths.
- **Optimal identification excitation** An elementary method was developed for calculating an identification drive PSD functions specifically suited to the dynamic behaviour of the test rig. These rig specific identification drive signal PSD functions improve model accuracy and model stability.

Further research in QanTiM specific repeatability functions will provide the simulation engineer with valuable information with which to assess test rig integrity prior to modelling.

A field that poses potential for further investigation concerns the system analogue to digital sampling rate. The use of a localised sampling rate is suggested. This implies a constant ratio between sampling rate and signal frequency. It is however not possible to sample at various rates, a high sampling rate would thus be used and the signals then decimated prior to modelling and simulation. As a first implementation, a scheme similar to that presented for split spectra modelling is suggested. Each separate model will however utilise a different sampling rate. It is proposed that the use of such localised sampling rates would improve model accuracy and eliminate errors related to numerical instability.

Further research into optimal identification excitation signals is most definitely necessary. The effect of excitation signal characteristics proved extremely significant and yet it is the part of the simulation procedure, which involves the most *black magic*. An automated excitation routine would greatly improve the versatility and ease of use of the existing QanTiM package.

The concept of a fixed simulation bandwidth has been implemented within QanTiM, but additional research is required into modelling and simulating with a bandwidth broader than that of the desired response data.

At present it appears that non-linear modelling capabilities are however the most likely to have a significant effect on simulation results. Research into non-linear system identification and response reconstruction is presented formally in part II of this thesis.